

## EQUATION OF THE GROWTH RATE OF FROST FORMING ON COOLED SURFACES

H. W. SCHNEIDER

Institut für Schiffs- und Anlagenbetriebstechnik, 2000 Hamburg 1, Stiftstraße 69, W. Germany

(Received 24 June 1977)

**Abstract**—Based on accurate measurements of a cooled tube the frost thickness turns out to be independent of the variables commonly significant on mass transfer, such as Reynolds number and vapor pressure difference. The frost thickness rather follows the law of crystal growth which is largely affected by the ratio of supersaturation and conduction of the heat of sublimation delivered when the molecule is incorporated into the lattice. The equation derived from a simplified model, satisfies the measured values with a probable error of  $\pm 3.7\%$ . The calculated values are in good agreement with experimental results of previous investigators even in the case of different geometrical shape and arrangement of the cooled surface as well as different kind of flow.

### NOMENCLATURE

$A_i$ ,	cross-section of ice needle;
$C_0 + C_5$ ,	constants;
$F_s$ ,	function defined by equation (12);
$\Delta h_s$ ,	specific latent heat of sublimation;
$k_i$ ,	thermal conductivity of water-ice;
$m, \dot{m}$ ,	mass, mass flow rate;
$n$ ,	exponent;
$p$ ,	partial vapor pressure of air;
$p'$ ,	vapor pressure of saturated air;
$p'_f$ ,	pressure of saturated vapor at frost surface temperature;
$Q_s$ ,	total heat delivered by sublimation;
$Re$ ,	Reynolds number;
$R_s$ ,	ratio of supersaturation;
$t$ ,	air temperature;
$t_f$ ,	frost surface temperature;
$t_M$ ,	melting point temperature of water-ice;
$t_w$ ,	wall temperature;
$x_f$ ,	frost thickness.

### Greek symbols

$\Pi$ ,	ratio defined by equation (10);
$\rho_i$ ,	density of water-ice;
$\tau$ ,	time;
$\phi$ ,	relative humidity.

### 1. INTRODUCTION

WHEN heat exchanger surfaces are cooled at temperatures of below  $0^\circ\text{C}$ , usually frost formation occurs. This phenomenon common in the field of refrigerating and air-conditioning techniques has an adverse effect upon heat transfer and pressure loss. Hence the growth rate of frost holds a key-position considerably influencing both the thermal resistance of the frost layer and the pressure drop of the air cooler. Until now there has been a need of a relationship which allows prediction of the frost thickness according to the environmental conditions. Experiments will be presented resulting in an equation capable of predicting the frost growth rate.

### 2. ACTUAL KNOWLEDGE

It is known from previous investigations [1, 2] that the frost growth rate varies with time according to a parabola-like function. The frost thickness increases with decreasing temperature of the cooled surface and with increasing relative humidity of the air stream. Special emphasis should be put on the result of Kamei *et al.* [2] who found the frost growth rate to be independent of the Reynolds number. This finding is verified in a later investigation by Yonko and Sepsy [1].

### 3. SCOPE OF EXPERIMENTAL RUNS

For experiments a cylindrical tube of 47.5 mm O.D. was used. The tube was placed in a closed-loop wind tunnel, where the dominating variables, such as temperature, relative humidity and velocity of the air stream as well as the surface temperature of the cooled tube could be held constant with great accuracy over a long period of time.

The tests were run over a range of air velocities from 1.2 to 10 m/s. It was possible to vary the air temperature from  $5$  to  $15^\circ\text{C}$  and the relative humidity from 50 to 100%. The temperature of the cooled tube was varied from  $-5$  to  $-30^\circ\text{C}$ . Based on these conditions the frost surface temperature, hardly accessible for accurate measurements, usually took the value of  $0^\circ\text{C}$ .

### 4. EXPERIMENTAL RESULTS

In Fig. 1 the frost thickness  $x_f$  is plotted against time  $\tau$  as a function of temperature  $t_w$  of the cooled tube wall. Different symbols have been chosen to represent each measured value according to its Reynolds number. The illustration shows that in spite of different Reynolds numbers, values taken at the same wall temperature  $t_w$  can be represented with good accuracy by one curve. Thus, the findings of Kamei *et al.* [2] and Yonko and Sepsy [1] are verified.

A result causally similar to that one above is shown in Fig. 2, where the frost thickness  $x_f$  is plotted once

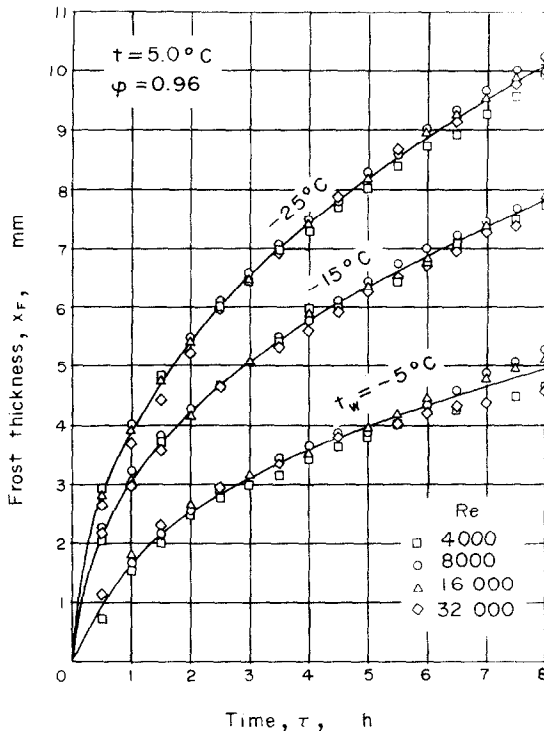


FIG. 1. Effect of Reynolds number and wall temperature on frost growth rate.

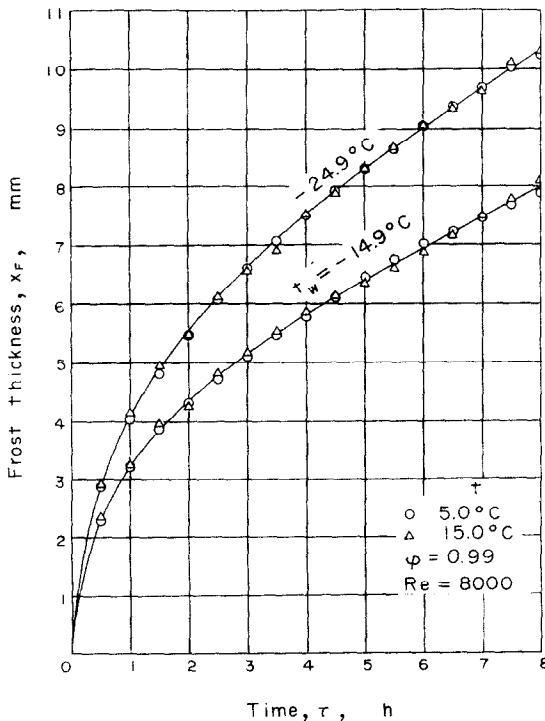


FIG. 2. Effect of humidity content and wall temperature on frost growth rate.

more as a function of the wall temperature  $t_w$ . In opposition to Fig. 1 each curve represents measurements carried out at different air temperatures  $t$ . The air flow was nearly saturated in all four cases. This means that the vapor pressure difference existing between the air stream and the frost surface, at air

temperatures of  $15^\circ\text{C}$  is nearly two times as high as at  $5^\circ\text{C}$ . According to the mass-transfer equation, one should expect the values obtained at the same air temperature to form one curve. But in fact, those values do coincide which were taken at the same wall temperature.

These two striking facts will be explained later on. For the present the result should be kept in mind, that the frost growth rate is independent of both Reynolds number and vapor pressure difference between air stream and frost surface.

##### 5. CORRELATION OF EXPERIMENTAL RESULTS

It seems not to be evident, that the wall temperature  $t_w$  should greatly affect the frost growth rate, because this value only exists on the cooled side of the frost layer. The temperatures prevailing in the interior of the layer are above  $t_w$ , continuously rising up to the temperature  $t_F$  of the frost-air interface.

In the case of the four runs shown in Fig. 2, the frost surface temperature reached its upper value of  $0^\circ\text{C}$  within an average time of 2 h after starting the test. At this time the temperature difference  $t_F - t_w$ , too, was equal for two runs at a time, being  $14.9$  and  $24.9^\circ\text{C}$  respectively. Therefore the temperature difference  $t_F - t_w$  existing in the whole range of the frost layer must be considered as a significant variable with regard to the frost growth rate.

In order to get a more complete insight into the mechanism of frost formation, a single needle of ice will be regarded, its length being  $x_F$  and its cross-section  $A_1$  (see Fig. 3). The portion of water-vapor  $dm$  sublimates

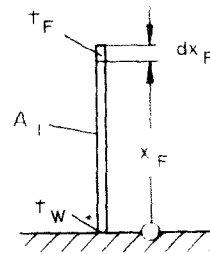


FIG. 3. Model of frost needle.

at its top, causing the length of the needle to increase according to the portion  $dx_F$ . Thus the quantity of heat  $dQ_S$  delivered by condensation into the solid phase, is

$$dQ_S = \Delta h_S \cdot \rho_i \cdot A_1 \cdot dx_F. \quad (1)$$

In equation (1),  $\Delta h_S$  represents the specific latent heat of sublimation,  $\rho_i$  the density of water-ice. In addition to the heat transferred by convection, the quantity  $dQ_S$  is conducted throughout the needle by means of the temperature difference  $t_F - t_w$ . If one adopts the temperature distribution inside the needle to be linear, which approximately holds true for the first 10 h after starting the test [3], one gets

$$dQ_S = \frac{C_0 \cdot k_i}{x_F} \cdot A_1 \cdot (t_F - t_w) \cdot d\tau. \quad (2)$$

In equation (2)  $C_0 \cdot k_i$  represents that portion of the

thermal conductivity  $k_1$  of water-ice necessary to conduct the heat  $dQ_s$  through the needle. Combination of equations (1) and (2) yields

$$x_F = C_1 \left( \frac{k_1}{\Delta h_s \cdot \rho_1} \right)^{1/2} [\tau(t_F - t_W)]^{1/2} \quad (3)$$

where

$$C_1 = (2 \cdot C_0)^{1/2}. \quad (4)$$

Since the value of  $C_0$  is unknown, the constant  $C_1$  has to be evaluated by experiment.

Looking at equation (3) the relationship concerning temperature difference  $t_F - t_W$  and time  $\tau$ , may be expressed by power functions, the value of the exponent being 0.5 in both cases. If this holds, will now be verified by measurements.

The experimental results, when plotted against time  $\tau$  on log-log paper (see Fig. 4) clearly show, that the

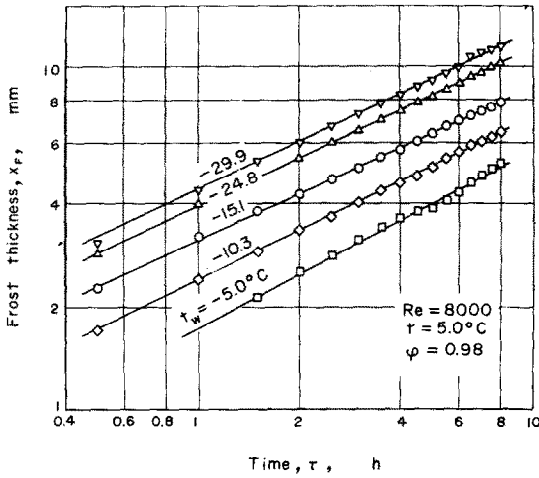


FIG. 4. Variation of frost thickness with time at different wall temperatures.

frost thickness  $x_F$  may be represented by a set of straight lines. The exponents of  $\tau$  being different for each run, the extreme values do not exceed the range between 0.43 and 0.51. Since it was not possible to find out a distinct dependence between these exponents and other parameters of the tests, an average value has been adopted being 0.47. It is only 6% below the value predicted by equation (3).

Figure 5 illustrates the influence of the temperature difference  $t_F - t_W$ , existing across the interior of the frost layer. The frost thickness  $x_F$  has been divided by the functions  $\Pi^{0.25}$  and  $F_r$ , which will be discussed later on. The values of  $x_F$  line up well along straight lines with logarithmic coordinates. The exponent of  $t_F - t_W$  takes the value 0.49, well confirming equation (3).

Equation (3) has been developed by means of a simplified model of the frost layer, not considering several processes which take place in the interior and at the surface of the frost layer. This concerns the period, in which the frost deposit initially existing of single needles which are orientated normal to the tube wall, begins to mesh. This concerns, too, the migration

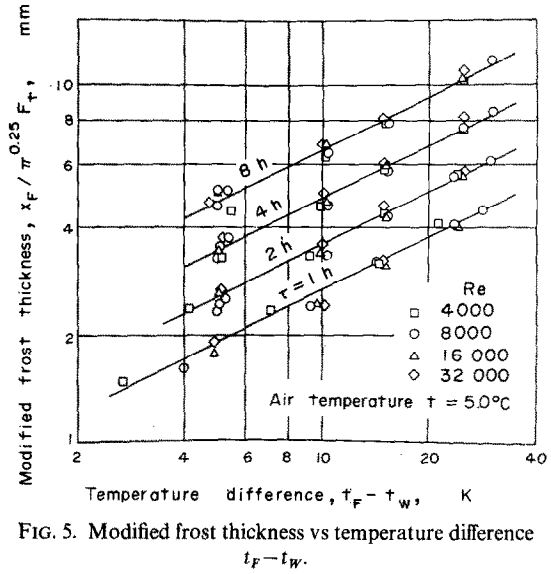


FIG. 5. Modified frost thickness vs temperature difference  $t_F - t_W$ .

of water vapor inside the permeable structure and the processes of local melting and condensation that cause the temperature distribution to deviate from its linear shape [3]. Evidently these processes are taken sufficiently into consideration by adapting the exponents of  $\tau$  and  $t_F - t_W$  to the real situation. This will be verified by measurements of different investigators, particularly by the long-time runs of Schropp [4]. Thus equation (3) passes into a non-dimensionless form which will be retained with regard to the advantages explained above.

$$x'_F = C_2 \left[ \frac{k_1}{\Delta h_s \cdot \rho_1} \cdot \tau \cdot (t_F - t_W) \right]^{1/2} \times \left( \frac{\tau}{1h} \right)^{-0.03} \cdot \left( \frac{t_F - t_W}{1K} \right)^{-0.01} \quad (5)$$

In equations (3) and (5) the relative humidity of the air stream has not been taken into account. Hence equation (5) only holds for a certain value of relative humidity. It shall be assumed that  $C_2$  has been evaluated for the case of saturated humid air. This may be indicated in equation (5) by using  $x'_F$  instead of  $x_F$ .

The mass-transfer rate  $\dot{m}$  to crystals growing from solution according to McCabe [5] is a function of the ratio of supersaturation  $R_s$ .

$$\dot{m} = C_3 \cdot (R_s - 1)^n. \quad (6)$$

Since for crystals growing from the gaseous phase the same mechanism is true, equation (6) may be used. Composing  $R_s$  of the vapor pressures involved in the problem, the quantity of water vapor condensing at the top of a frost needle is

$$m = C_4 \cdot \left( \frac{p - p'_F}{p'_F} \right)^n = C_5 \cdot x_F \quad (7)$$

where  $p$  represents the partial vapor pressure of the air flow and  $p'_F$  the pressure of saturated vapor at the temperature  $t_F$  of the frost surface. The values of  $C_4$  and  $n$  have to be evaluated from the test data. Remembering the relationship between length  $x_F$  of a

frost needle and  $m$  to be linear, this is expressed, too, by equation (7),  $C_5$  being a constant factor.

In the case of saturated air  $p$  is replaced by the pressure  $p'$  of saturated vapor. Thus equation (7) passes into

$$m' = C_4 \cdot \left( \frac{p' - p'_F}{p'_F} \right)^n = C_5 \cdot x'_F \quad (8)$$

Combination of equations (5), (7) and (8) yields

$$x_F = C_2 \left[ \frac{k_1}{\Delta h_S \cdot \rho_1} \cdot \tau \cdot (t_F - t_W) \right]^{1/2} \times \left( \frac{\tau}{1h} \right)^{-0.03} \left( \frac{t_F - t_W}{1K} \right)^{-0.01} \Pi^n \quad (9)$$

where

$$\Pi = \frac{p - p'_F}{p' - p'_F} \quad (10)$$

In Fig. 6 this relationship is illustrated at different hours after starting the test. The values of  $x_F$ , divided by functions  $[(t_F - t_W)/1K]^{0.49}$  and  $F_t$ , line up well along straight lines when plotted on log-log paper. The exponent of  $\Pi$  takes the value

$$n = 0.25 \quad (11)$$

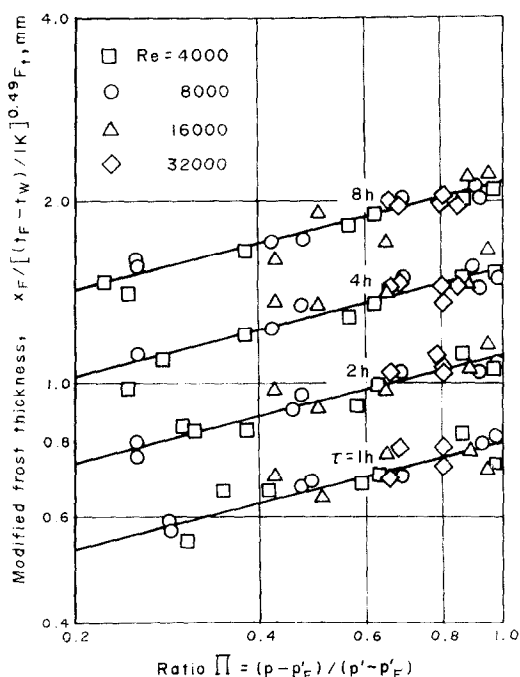


FIG. 6. Modified frost thickness as a function of ratio  $\Pi$ .

The frost thickness decreases [see equation (9)] when the temperature difference  $t_F - t_W$  existing between frost surface and tube wall tends to zero. At wall temperatures not far below the melting point, this is true only with restriction as the mechanism of frost formation obviously undergoes a transition. When the air temperature is considerably above  $0^\circ\text{C}$  the frost surface fast becomes humid. Condensate soaks into the porous frost structure and freezes, forming a layer of ice. Upon that new water-vapor condenses and freezes.

At these conditions the rate of mass transfer to the surface is important due to the high vapor pressure gradient even at lower relative humidities. Therefore the increase in frost thickness is more important as it might be expected by the temperature difference  $t_F - t_W$ . This influence on the frost growth rate may be taken into account by an empirical function

$$F_t = 1 + 0.052 \frac{t - t_M}{t_M - t_W} \quad (12)$$

where  $t_M$  represents the melting point temperature of water-ice. If the air temperature is below  $0^\circ\text{C}$ , the value of  $F_t$  consequently must be set unit.

The complete equation representing the frost growth rate may then be written

$$x_F = 0.465 \left[ \frac{k_1}{\Delta h_S \cdot \rho_1} \cdot \tau \cdot (t_F - t_W) \right]^{1/2} \times \left( \frac{\tau}{1h} \right)^{-0.03} \left( \frac{t_F - t_W}{1K} \right)^{-0.01} \Pi^{0.25} F_t \quad (13)$$

Equation (13) satisfies the measured values with a maximum error of  $\pm 10\%$  in the range of  $1 \leq \tau \leq 8$  h. The probable error is  $\pm 3.7\%$ , slightly exceeding the error of measurements. Even in case of those runs, which were extended to 28 h, the deviations are in the indicated range.

A reduced reliability of equation (13) is forthcoming in the range of  $\tau < 1$  h. Cinephotomicrographic studies performed by Biguria and Wenzel [6] show, that a continuous transition of the mechanism of heat and mass transfer is characteristic for the first period of frost formation which takes place within 15–45 min after starting the test. Consequently a different relationship may be true of the early stages of deposition than of the subsequent quasi steady state, to which this presentation refers.

Equation (13) enables at least estimation of the frost growth rate of any given two-component system unless it is supersaturated. It was not possible to verify the accuracy of equation (13) in these cases, as qualified measurements were not available.

## 6. INTERPRETATION OF RESULTS

When a crystal grows from the gaseous phase the molecules which form the lattice initially are adsorbed at the crystal surface. Centers of preferred adsorption are represented by corners, edges and interfaces of phases. In most cases the molecules corresponding to their temperature dispose of thermal energy, sufficient to change the place of initial adsorption. Migration along the surface takes place until the local position is reached where the molecule is built into the lattice with maximum decrease of the interfacial energy. Favourable conditions of mass transfer are given in the boundary layer of thin dendrites. Therefore the supposition may be allowed, that the processes which take place at the interface of the phases represent the controlling effects on the mass-transfer rate.

This kind of interpretation would be incomplete unless another process is taken into account which

occurs, too, at the early stages of frost formation. According to the theory of nucleation [7] a certain number of molecules is necessary to form through cluster formation a new embryo. The probability of this process depends on the quantity of water vapor molecules present in the neighbourhood of the cooled surface. Nucleation therefore means consumption of water vapor molecules which are continuously replaced by new molecules coming out of the bulk flow. This transfer process depends on the vapor pressure difference between air stream and cooled surface and on the Reynolds number. The explanation agrees with cinephotomicrographic studies carried out by Biguria and Wenzel [6] who observed an increase of nucleation with rising air velocity. This explanation is justified, too, by the observation [8, 9] that the distribution of frost needles along the circumference of a cylinder corresponds to that of the transfer coefficient.

Thus the mass-transfer equation still rests valid even in the case of frost formation. Instead of the growth rate, the rate of nucleation is affected by a change of the transfer conditions resulting in a corresponding change of the frost density. The frost thickness on the other side depends on the principles of crystal growth. The latter is controlled by the ratio of supersaturation represented by the function  $\Pi$ . It depends, too, on the conditions prevailing to conduct the heat of sublimation across the frost layer.

In this way the results presented at the beginning could be explained which showed the frost growth rate to be independent of the Reynolds number as well as of the vapor pressure difference between air stream and frost surface. For the same reason the frost thickness is independent of the position along the circumference of the tube. This observation agrees with observations of Biguria and Wenzel [6] who studied a flat plate.

#### 7. COMPARISON WITH PREVIOUS INVESTIGATIONS

In Fig. 7 values calculated by equation (13) are compared with measurements of the frost thickness obtained by different authors.

Frost formation and heat transfer on a cylinder surface (89.5 mm O.D.) in cross flow was studied by Trapanese [10]. The same was done by Prins [8] using a staggered tube bank (38.5 mm O.D.). Measurements concerning a horizontal tube (50 mm O.D.) in natural convection were carried out by Schropp [4]. The tests were run over a range of 250–300 h presenting the opportunity to verify equation (13) for long periods of time. Schropp's investigation confirms that it has been correct to adopt the value of 0.47 for the exponent of time  $\tau$  [see equation (5)]. The original value of 0.5 in contrast would have produced average deviations of 17%. Frost formation on a cylinder (32 mm O.D.) forming an annulus with a concentrically arranged tube was investigated by Kamei *et al.* [2], while the experiments of Lotz [11] are concerned with an extended surface coil.

Most of these values are in the indicated range of  $\pm 10\%$ . This is true without restriction for all tests, in which the temperature of the frost-air interface is

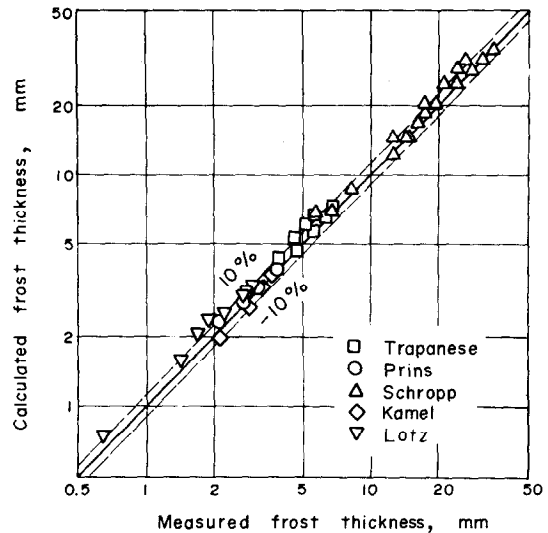


FIG. 7. Comparison of calculated and measured values of frost thickness.

known [8, 2]. Maximum deviation appears in the case of Lotz's measurements where both frost surface temperature and temperature of the cooled fin were unknown and have been evaluated by approximation.

Although the diameter of the test tubes varies in the range of 4:1, no influence on frost formation is forthcoming. The curvature of the cooled surface therefore seems to be of subordinate importance.

The test conditions of the above mentioned authors being extremely different to some extent verify the considerations made above. Hence the frost thickness is independent of the ambient conditions of mass transfer. The same is true of the geometrical shape of the flow channel as well as of the kind of flow.

#### 8. CONCLUSIONS

The frost thickness turns out to be independent of the conditions commonly significant for mass transfer such as arrangement of the test surface, vapor pressure difference between air stream and frost surface and Reynolds number. On the other side ratio of supersaturation and capability of frost to conduct the heat of sublimation delivered when the molecule is built into the lattice, both effects of crystal growth, largely affect the frost growth rate.

The frost thickness may be represented by a simplified model to be the square root of time and temperature difference between frost surface and cooled wall. The various processes occurring at the frost-air interface and in the neighbourhood of the cooled wall are taken into account by adjusting the exponents of both variables. The effect of relative humidity was taken into consideration corresponding to the theory of crystal growth by the ratio of supersaturation.

The derived equation satisfies the measured values with a probable error of  $\pm 3.7\%$ , the maximum error being  $\pm 10\%$ . The calculated values are in good agreement with experimental results of different test

arrangements. Thus previous considerations were confirmed.

As equation (13) includes all properties involved into the problem application to any given non-saturated two-component system seems possible.

*Acknowledgement*—The measurements of this study were sponsored by the Deutsche Forschungsgemeinschaft.

#### REFERENCES

1. J. D. Yonko and C. F. Sepsy, An investigation of the thermal conductivity of frost while forming on a flat horizontal plate, Preprint No. 2043, ASHRAE 74th Annual Meeting, Minneapolis (1967).
2. S. Kamei, T. Mitzushina, S. Kifune and T. Koto, Research on the frost formation in a low temperature cooler condenser, *Japan Sci. Rev.* **2**, 317–326 (1952).
3. H. W. Schneider, Temperature distribution in a frost layer formed on a cylindrical tube in cross flow, *Annexe au Bull. de l'Inst. Int. du Froid*, 425–431 (1969–7).
4. K. Schropp, Untersuchungen über die Tau- und Reifbildung an Kühlrohren in ruhender Luft und ihr Einfluß auf die Kälteübertragung, *Z. Ges. Kälteind.* **42**, 81–85, 126–131, 151–154 (1935).
5. W. L. McCabe and J. C. Smith, *Unit Operations of Chemical Engineering*, 2nd edn, p. 768, McGraw-Hill, New York (1967).
6. G. Biguria and L. A. Wenzel, Measurement and correlation of water frost thermal conductivity and density, *I/EC Fundamentals* **9**, 129–138 (1970).
7. M. Volmer, *Kinetik der Phasenbildung*, Steinkopff, Dresden und Leipzig (1939).
8. L. Prins, Wärme- und Stoffübertragung in einem quer angeströmten, bereifenden Luftkühler, *Kältetechn.* **8**, 160–164, 182–187 (1956).
9. H. W. Schneider, Der Wärmeübergang an einem bereifenden, quer angeströmten Rohr, Diss. Universität Stuttgart (1972).
10. G. Trapanese, Ricerche sperimentali sulla trasmissione del calore nei tubi brinati, Estr. d.: Atti del X Congresso Naz. del Freddo Padova (1961).
11. H. Lotz, Wärme- und Stoffaustauschvorgänge in bereifenden Lamellenrippen-Luftkühlern im Zusammenhang mit deren Betriebsverhalten, Diss. Techn. Hochschule Aachen (1968).

#### EQUATION DE LA VITESSE DE CROISSANCE DU GIVRE SUR DES SURFACES FROIDES

**Résumé**—Des mesures précises sur un tube refroidi montrent que l'épaisseur de la couche de givre est indépendante des paramètres spécifiques du transfert de masse, c'est à dire du nombre de Reynolds et de la différence de pression partielle de vapeur d'eau entre le courant d'air et la paroi froide. Elle obéit par contre à la loi de formation du cristal qui dépend tout d'abord du rapport de sursaturation et des conditions de passage de la chaleur de sublimation dégagée à l'incorporation des molécules dans l'édifice cristallin. L'équation établie à l'aide d'un modèle simple représente des données expérimentales avec une erreur probable de  $\pm 3,7\%$ . Les valeurs calculées sont en bon accord avec les résultats expérimentaux des auteurs précédents, même dans le cas de formes et de dispositions différentes de la surface refroidie ainsi que de types différents d'écoulement.

#### EINE GLEICHUNG FÜR DAS ANWACHSEN VON RAUHREIF AUF GEKÜHLTEN OBERFLÄCHEN

**Zusammenfassung**—Im Gegensatz zur Theorie der Stoffübertragung erweist sich die Reifdicke aufgrund genauer Messungen an einem gekühlten Rohr als unabhängig von der Reynolds-Zahl und von der Dampfteildruckdifferenz zwischen Strömung und gekühlter Rohrwand. Sie unterliegt vielmehr den Gesetzmäßigkeiten der Kristallbildung, für die in erster Linie das Übersättigungsverhältnis und die Bedingungen für die Fortleitung der beim Einbau in das Kristallgitter freiwerdenden Wärme maßgebend sind. Die anhand eines einfachen Modells entwickelte Gleichung gibt die eigenen Messungen mit einem wahrscheinlichen Fehler von  $\pm 3,7\%$  wieder. Ein Vergleich mit fremden Versuchsergebnissen führt selbst bei erheblichen Unterschieden von Gestalt und Anordnung der gekühlten Flächen sowie Art der Strömung auf gute Übereinstimmung.

#### УРАВНЕНИЕ ДЛЯ СКОРОСТИ НАРАСТАНИЯ ИНЕЯ НА ОХЛАЖДАЕМЫХ ПОВЕРХНОСТЯХ

**Аннотация** — Точные измерения на охлаждаемой трубке показали, что толщина инея не зависит от таких переменных, как число Рейнольдса и разность давлений пара, которые обычно имеют большое значение при массообмене. Скорее нарастание инея подчиняется закономерностям роста кристаллов, где большую роль играют коэффициент сверхнасыщения и теплота сублимации, выделяемая при присоединении молекулы к решетке кристалла. Выведенное на основании упрощенной модели уравнение хорошо описывает измеренные значения в пределах погрешности  $\pm 3,7\%$ . Теоретические результаты хорошо согласуются с экспериментальными данными предыдущих исследователей даже в случае другой геометрии охлаждаемой поверхности и ее расположения, а также других видов течения.